

Light reflection and transmission by a temperate snow cover

Donald K. PEROVICH

*Engineer Research and Development Center, US Army Cold Regions Research and Engineering Laboratory,
72 Lyme Road, Hanover, New Hampshire 03755-1290, USA
E-mail: donald.k.perovich@erdc.usace.army.mil*

ABSTRACT. An understanding of the reflection and transmission of light by snow is important for snow thermodynamics, hydrology, ecology and remote sensing. Snow has an intricate microstructure replete with ice/air interfaces that scatter light. Spectral observations of light reflection and transmission, from 400 to 1000 nm, were made in temperate snowpacks, under cold and under melting conditions. The optical observations were made using a dual-detector spectroradiometer. One detector was placed above the snow surface to monitor the incident and reflected solar irradiance, and the second detector was placed at the base of snow cover to measure downwelling irradiance. The optical measurements were supplemented by a physical characterization of the snow, including depth, density and an estimate of grain size. In general, transmitted light levels were low and showed a strong spectral dependence, with maximum values between 450 and 550 nm. For example, a 10 cm thick snow layer reduced visible transmission (500 nm) to about 5% of the incident irradiance, and infrared transmission (800 nm) to less than 1%. Extinction coefficients were in the range $3\text{--}30\text{ m}^{-1}$, and tended to decrease slightly as the snow aged and increase as snow density increased.

INTRODUCTION

At visible wavelengths, snow is a highly scattering optical medium (Warren, 1982). It is well known that even a thin snow cover is bright and white, reflecting most of the incident sunlight and transmitting little. Snow grains are small, sub-millimeters to millimeters in size, and a snowpack has a multitude of air/ice interfaces to scatter light. An understanding of the interaction of solar radiation with snow is an essential element to a diverse set of research areas, including investigations of climate feedbacks (Barry, 1996; Nolin and Stroeve, 1997), snow ecology (Smith and others, 1992; Thomas and Duval, 1995; McKenzie and others, 1998), snow chemistry (Wolff and others, 2002), hydrology and remote-sensing interpretation (Warren and others, 1998; Jin and Simpson, 2001; Stroeve and Nolin, 2002). Solar radiation is a key component of the energy budget of snow. Indeed, detailed snow thermodynamic models need information on absorption of solar radiation with depth in the snowpack (Brandt and Warren, 1993; Beaglehole and others, 1998). Spectral albedos and bidirectional reflectance distribution functions are needed to interpret visible and near-infrared remote-sensing signatures. The amount and spectral distribution of light transmitted through snow is of biological importance in both terrestrial and marine environments.

Because of energy budget concerns, hydrological impacts and potential climatic implications, there is a rich literature of observational and theoretical work examining spectral- and wavelength-integrated snow albedos. Many previous snow studies have been conducted in polar (Grenfell and Maykut, 1977; Grenfell and Perovich, 1984; Grenfell and others, 1994; Beaglehole and others, 1998; Warren and others, 1998; Gerland and others, 1999; Hamre and others, 2004) or alpine settings (Grenfell and others, 1981; Nolin and others, 1994; Painter and Dozier, 2004). While there are abundant studies of light reflection, there are far fewer studies of light transmitted through snow (Giddings and LaChapelle, 1961; Brandt and Warren, 1993; Beaglehole

and others, 1998; Gerland and others, 2000; Hamre and others, 2004). Transmission measurements through snow are notoriously difficult. Light levels beneath even a modest 10 cm deep snowpack are only a few percent in the visible and <1% in the near-infrared. There are also spectral complications; while reflected light is relatively 'white' uniform at all wavelengths, transmitted light has a strong spectral dependence. Consequently, light leakage from one wavelength to another within the instrument is a serious experimental concern. Finally, it is difficult to insert a sensor into a snowpack to measure light transmission without disturbing the snowpack. Either the sensor obscures the light field or its placement possibly creates pathways in the snow for spurious light transmission.

This paper presents observations of light reflection and transmission by snow made in a quasi-laboratory setting in Hanover, NH, USA. In these measurements a spectroradiometer was embedded in the ground before the snow fell. Observations are presented of spectral albedos and transmittances for a range of snow depths, densities, grain sizes and wetnesses. Extinction coefficients were calculated using a two-stream radiative-transfer model. Also, profiles of transmittance as a function of snow depth were used to determine asymptotic extinction coefficients. The effects of snow depth, new snow, melting snow and snow density on albedo and transmittance are investigated.

INSTRUMENTS AND METHODS

The primary aim of this work was to measure the spectral distribution of light transmitted through a snow cover. One of the difficulties of making transmission measurements is disturbing the snow while installing the detector. To avoid this problem, an idea from Giddings and LaChapelle (1961) was revisited. A 2.4 m by 2.4 m horizontal plywood platform was built (Fig. 1). The plywood was painted black to simplify the bottom boundary condition so that the upwelling radiation at the bottom of the snowpack was zero. An



Fig. 1. The experimental set-up consisted of a 2.4 m × 2.4 m black plywood base with a detector mounted in the center (arrow 1) that measured transmitted irradiance. Incident and reflected irradiance were measured using a second detector that was mounted on a tripod (arrow 2).

upward-looking spectroradiometer was placed in the middle of this black platform to measure the transmitted spectral irradiance. A second, matched spectroradiometer was mounted above the platform and was used to measure the incident and reflected irradiance. This spectroradiometer was mounted on a 1.5 m long arm and placed on a tripod to minimize shadowing and for easy leveling. Calibration and intercomparison of the two spectroradiometers were performed in the field.

The spectroradiometers (Spectron Engineering SE-590) were photodiode-array instruments with rapid response times, so that a full spectrum could be measured in a few seconds. It typically took <1 min to measure a sequence of incident, reflected and transmitted irradiance spectra. Hemispherical cosine collectors were used to obtain the appropriate instrument field of view for irradiance measurements. Spectral measurements were made at 200 discrete wavelengths between 400 and 1000 nm, with a spectral resolution of 5 nm. The noise equivalent power of the instrument, with cosine collector, was $10^{-9} \text{ W cm}^{-2} \text{ nm}^{-1}$.

In principle, the notion was simple: use this set-up to make a series of measurements of spectral incident, reflected and transmitted irradiance as the snow depth increased during a snowfall. In practice this proved to be difficult. Often it snowed at night, when optical measurements were impossible. In some cases, when it did snow during the day, the snowfall was so intense that the equipment failed. Because of these difficulties, observations were typically made after a snowfall. A set of optical observations consisted of scans of spectral incident, reflected and transmitted irradiance. A measurement sequence consisted of several sets with a few centimeters of the snow cover incrementally stripped off between each set. This produced profiles of transmission as a function of snow depth, as well as albedos and transmittances.

The optical measurements were supplemented by a physical characterization of the snow. Snow depth (H) and density were measured. Snow grain size and grain shape

were subjectively determined using a scale and eyepiece as well as photographs. A qualitative assessment of the snow wetness was made (e.g. dry, icy, barely packable and wet). The site was photographed (Fig. 2) to preserve a general sense of snow conditions, and microphotographs of snow grains were also taken. Measurements were intentionally made only under cloudy skies with the solar disk either barely visible or not visible. These conditions were selected to minimize the direct solar beam contribution to the incident radiation field, simplifying the interpretation of the measurements.

The measurements were made at the Cold Regions Research and Engineering Laboratory in Hanover, NH (43.6° N, 72.3° W; elevation 150 m) during the winters of 1994, 1996, 1997 and 2000. Hanover has a four-season, highly changeable climate, with snowfall common from mid-November through to the end of March. Snowfalls range from a few centimeters to tens of centimeters. Hanover is a small town in a rural location, and there were probably more contaminants in the snowpack than in the isolated polar regions that are often the location for snow studies (Grenfell and others, 1981, 1994, 2002; Grenfell and Perovich, 1984; Beaglehole and others, 1998; Warren and others, 1998).

This method had the advantage of being able to measure, easily and quickly, the reflected and transmitted light without disturbing the snow. It was also possible to obtain measurements on a fairly homogeneous snow cover. The drawbacks of the set-up were a lack of portability, the impossibility of surveying a wide range of conditions and the need to wait for snowfall.

THEORETICAL CONSIDERATIONS

From the measured sets of incident ($F_{\downarrow}(0, \lambda)$), reflected ($F_{\uparrow}(0, \lambda)$) and transmitted ($F_{\downarrow}(H, \lambda)$) spectral irradiance, it is straightforward to calculate the albedo and the transmittance. At a particular wavelength, λ , the albedo, α , is simply

the fraction of the incident downwelling irradiance that is reflected or, more formally,

$$\alpha = \frac{F_{\uparrow}(0, \lambda)}{F_{\downarrow}(0, \lambda)}. \quad (1)$$

Similarly, the transmittance, T , is the fraction of the incident downwelling irradiance that is transmitted through the snow cover of depth H , or

$$T = \frac{F_{\downarrow}(H, \lambda)}{F_{\downarrow}(0, \lambda)}. \quad (2)$$

The albedo is the most significant and commonly measured optical property of the snow. Both the albedo and the transmittance are considered apparent optical properties. They depend not only on the optical properties of the snow, but also on parameters such as the snow depth, illumination and boundary conditions. More fundamental are the inherent optical properties that depend only on the medium. These are the spectral absorption coefficient (k_{λ}), the scattering coefficient (σ_{λ}) and the single-scattering phase function (g).

The albedo is straightforward to compute and to interpret. While the transmittance is also simple to compute, it is difficult to generalize, since transmittance is strongly dependent on snow depth. Knowing the transmittance for a particular case is of limited value. A more generalized quantity, such as the extinction coefficient, is needed. Inherent optical properties of the snow that do not depend on depth can be determined by combining observed albedos and transmittances using a radiative-transfer model. Many different radiative-transfer models for snow have been developed (Dunkle and Bevans, 1956; Bohren and Barkstrom, 1974; Warren and Wiscombe, 1980; Wiscombe and Warren, 1980; Warren, 1982; Stamnes and others, 1988; Mishchenko and others, 1999; Kokhanovsky and Zege, 2004; Grenfell and others, 2005).

The equation of radiative transfer developed by Chandrasekhar (1960) provides a complete theoretical treatment framework for the interaction of light with a snow cover:

$$\mu \frac{dI}{d\tau} = I(\tau, \mu, \phi) - S(\tau, \mu, \phi), \quad (3)$$

where I is the radiance, τ the optical depth, μ the cosine of the zenith angle and ϕ the azimuth angle. Scattering is considered in the S term. There are solutions to the equation of radiative transfer that can treat layers as thick or thin, scattering that is isotropic or anisotropic, and media that are scattering or absorbing or both. The price for this robust generality can be considerable computational complexity. The medium is defined by three inherent optical properties: the absorption coefficient (k_{λ}), the amount of absorption per unit distance; the scattering coefficient, the amount of scattering per unit distance; and the phase function, the angular dependence of scattering. Absorption coefficients have been determined for ice in the laboratory (Grenfell and Perovich, 1981; Warren 1984; Kou and others, 1993) and in the field (Askebjør and others, 1997; Warren and others, 2006). Results show significant differences in the magnitude of the absorption coefficients as well as the wavelength of minimum absorption (390 nm in the field vs 470 nm in the laboratory). Warren and others (2006) demonstrated that the laboratory absorption results were probably influenced by Rayleigh scattering. In addition, they explained that the typical peak albedo found, 430–500 nm, in many field observations is due to contributions from impurities such as

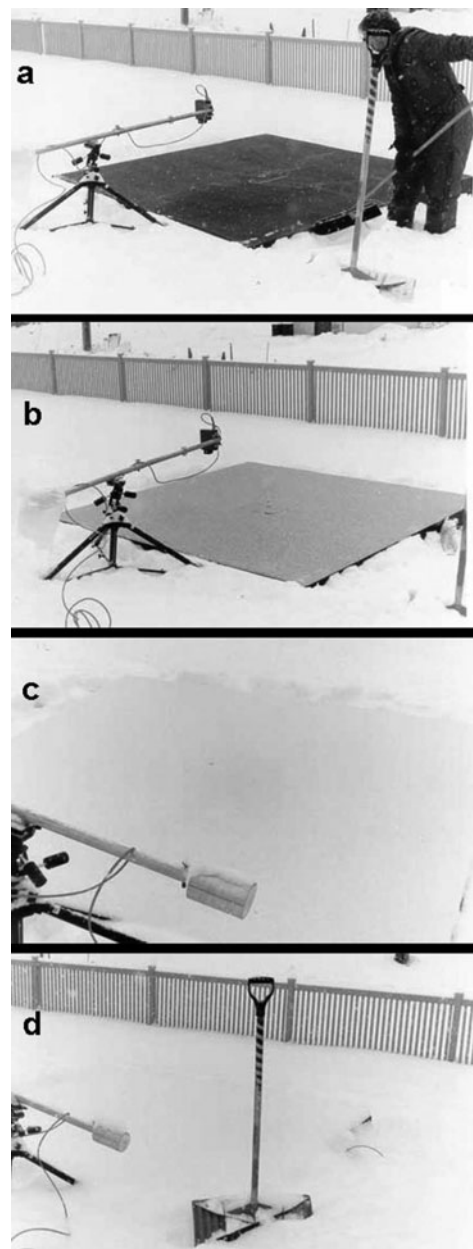


Fig. 2. Photographs of the black base taken over a 5 hour period during a snowfall. The snow depths were (a) 0 cm, (b) 0.5 cm, (c) 3 cm and (d) 8 cm.

soil, rock dust and algae. Basic scattering properties of snow are not known and are exceedingly difficult to measure directly. Forward and inverse models of Equation (6) have been developed for snow and sea ice to infer scattering properties from observations of albedo and transmittance (Bohren and Barkstrom, 1974; Warren and Wiscombe, 1980; Wiscombe and Warren, 1980; Perovich and Grenfell, 1982; Grenfell, 1991; Light, 2000).

There are models with simplifying assumptions that allow less complicated solutions to Equation (3). Dunkle and Bevans (1956) developed a 'two-stream', radiative-transfer model that computed the downwelling and upwelling irradiance in a medium. This model simplifies by assuming isotropic scattering, but can accurately treat optically thin layers. It has been used extensively in studies of the optical properties of sea ice and polar snow (Grenfell and Maykut, 1977; Grenfell, 1979; Perovich, 1990) and is the primary

Table 1. Physical and optical properties of selected cases

Wavelength	Property	Figure 4 4 Mar. 1994	Figure 6 12 Feb. 1997	Figure 6 12 Feb. 1997	Figure 7 12 Jan. 1996	Figure 7 18 Jan. 1996
<i>Physical</i>						
	Sky conditions	High, thin, lower broken	Complete cloud cover	Complete cloud cover	Complete cloud cover	Complete cloud cover
	Total depth (cm)	19	14	15.5	14.5	11
	Density (kg m ⁻³)	120	200	172	143	373
	Grain shape	Round	Round	Round	Columns	Round
	Grain diameter (mm)	0.25–0.5	0.5–1	0.5–1	1–3	0.5–1
<i>Optical</i>						
	Reflection coefficient (cm ⁻¹)	1.44	0.6	0.65	1.06	0.84
500 nm	Albedo	0.951	0.894	0.891	0.918	0.788
	Transmittance	0.027	0.045	0.038	0.047	0.034
	Extinction coefficient (cm ⁻¹)	0.062	0.065	0.074	0.077	0.219
600 nm	Albedo	0.941	0.896	0.894	0.911	0.795
	Transmittance	0.023	0.041	0.035	0.043	0.036
	Extinction coefficient (cm ⁻¹)	0.084	0.068	0.077	0.091	0.210
700 nm	Albedo	0.922	0.876	0.879	0.897	0.775
	Transmittance	0.012	0.028	0.021	0.029	0.027
	Extinction coefficient (cm ⁻¹)	0.132	0.095	0.104	0.129	0.243
800 nm	Albedo	0.889	0.809	0.839	0.862	0.709
	Transmittance	0.016	0.007	0.005	0.007	0.007
	Extinction coefficient (cm ⁻¹)	0.256	0.169	0.183	0.244	0.383

model used in this study. The solutions for upwelling (F_{\uparrow}) and downwelling (F_{\downarrow}) irradiances in the medium are

$$F_{\uparrow} = \frac{F_o \sinh[\kappa_{\lambda}(H-z)]}{\sinh\left[\kappa_{\lambda} + \sinh^{-1}\left(\frac{\kappa_{\lambda}}{r_{\lambda}}\right)\right]} \quad (4)$$

and

$$F_{\downarrow} = \frac{F_o \sinh\left[\kappa_{\lambda}(H-z) + \sinh^{-1}\left(\frac{\kappa_{\lambda}}{r_{\lambda}}\right)\right]}{\sinh\left[\kappa_{\lambda} + \sinh^{-1}\left(\frac{\kappa_{\lambda}}{r_{\lambda}}\right)\right]}, \quad (5)$$

where F_o is the incident irradiance, z is the depth within the medium, r_{λ} is the reflection coefficient (which is the two-stream version of the scattering coefficient) and κ_{λ} is the extinction coefficient defined as

$$\kappa_{\lambda} = \sqrt{k_{\lambda}^2 + r_{\lambda}^2}.$$

Equations (4) and (5) are substituted into Equations (1) and (2), along with the observed values of albedo, transmittance and snow depth. Using techniques developed by Grenfell and Maykut (1977), the resultant equations are iteratively solved to determine the reflection and extinction coefficients. This is the primary analysis method used in this paper.

For an optically thick layer, Equation (5) reduces to the familiar Bouguer–Lambert law, which predicts an exponential decrease in irradiance with depth

$$F_{\downarrow}(z, \lambda) = (1 - \alpha)F_{\downarrow}(0, \lambda)e^{-\kappa_{\lambda}z}. \quad (6)$$

The Bouguer–Lambert model is accurate in the interior of a semi-infinite medium with isotropic scattering. However, it is less precise for the near-surface layer, for thin slabs of snow or for non-isotropic scattering. Using this model, the extinction coefficient can be analytically determined from

measurements of albedo and transmittance, or from vertical profiles of irradiance within the medium.

Common to all radiative-transfer models is the concept of an asymptotic extinction coefficient. Deep within a multiply scattering medium such as snow, the radiative field is diffuse and extinction is described by

$$\kappa_{\lambda}(z) = \frac{1}{F_{\downarrow}(z, \lambda)} \frac{dF_{\downarrow}(z, \lambda)}{dz}. \quad (7)$$

This is essentially the Bouguer–Lambert law. Above this diffuse, asymptotic regime, Equation (7) is not appropriate, since the irradiance decreases faster than exponential and is dependent on the illumination and the boundary conditions (Bohren and Barkstrom, 1974).

There is a simplifying assumption for scattering in snow at visible and near-infrared wavelengths. The scatterers are the snow grains, which are much larger than the wavelength, and scattering is in the geometric optics regime. Also, the real portion of the index of refraction has little spectral variation in this wavelength region. Consequently, reflection coefficients are assumed to be constant with wavelength.

The following section presents observations of albedo and transmittance for a variety of snowpacks, including dry snow, wet snow, new snow and old metamorphosed snow. Extinction and reflection coefficients computed from albedos and transmittances are also provided for these cases. A series of profiles of spectral light transmission as a function of snow depth are discussed along with Bouguer–Lambert extinction coefficients.

RESULTS

During the winters of 1994, 1996, 1997 and 2000, measurements were made of 25 individual snow cases. Physical and

optical properties of selected cases are summarized in Table 1. Snow depths ranged from 9 to 25 cm. Snow densities were usually $100\text{--}200\text{ kg m}^{-3}$, with wet melting snow reaching values as high as 373 kg m^{-3} . New snow was typically a combination of needles, rounded grains and small plates, while the old snow was primarily rounded grains. On several occasions it was possible to monitor the evolution from freshly fallen snow to old metamorphosed snow to wet melting snow. The impact of adding a thin layer of new snow to an older snowpack was also examined.

Albedo and snow depth

For thin snow covers, albedo is strongly dependent on snow depth. Figure 2 is a photographic sequence of the black platform during a snowstorm as the snow depth increased from 0 to 0.5 to 3.0 to 8.0 cm. The snowpack density was 160 kg m^{-3} and it consisted of a mixture of dendritic crystals, with 25% needles and the remaining 75% exhibiting rounding of the angular parts. These had lengths of approximately 1 mm. The rapid increase in visible albedo with snow depth is evident in the photographs. When the snow depth was 0.5 cm, the underlying platform was clearly visible. At 3 cm the platform was barely distinguishable and by 8 cm the snow over the platform appears as white as the surrounding deeper snow.

This is illustrated quantitatively in Figure 3, where the spectral albedo at selected wavelengths is plotted as a function of snow depth. The rapid asymptotic increase of albedo with snow depth is evident at all wavelengths. There was a modest spectral difference in the asymptotic albedo due to spectral differences in the absorption coefficient of ice (Grenfell and Perovich, 1981; Warren, 1982). The increase in albedo was rapid from 0 to 4.5 cm, reaching values of 0.85–0.90, and relatively flat for deeper snow. Once the snow was deeper than approximately 10 cm, albedo increases were less than 5%.

Transmittance and extinction coefficient

From the standard optical measurements of incident, reflected and transmitted spectral irradiance, the spectral albedo and transmittance were directly calculated using Equations (1) and (2). Spectral albedos, transmittances and extinction coefficients from a 19 cm thick snowpack are presented in Figure 4. The measurements were made in March on a month-old snowpack consisting of 0.5 mm diameter rounded snow grains, with some of the grains aggregating into small (1–2 mm) clumps. Snow temperatures were below freezing and the density was 120 kg m^{-3} . Albedos (Fig. 4a) were large, with peak values of 0.95 at visible wavelengths declining to 0.85 in the near-infrared. These values are somewhat smaller (~ 0.04) than the Antarctic albedos reported by Grenfell and others (1994). The difference is probably due to the larger and rounder snow grains and higher levels of contaminants in the Hanover snowpack. In addition, there may be a small reduction due to the substrate: black in this experiment compared to optically thick snow in the Antarctic observations.

Transmittances (Fig. 4b) were much smaller than albedos. The uncertainty in the transmittance measurements was typically ± 0.001 . They exhibited a strong spectral dependence, ranging by more than an order of magnitude, with a peak of approximately 0.03 in the blue region of the spectrum. An inverse Dunkle and Bevens formulation (Dunkle and Bevens, 1956; Grenfell and Maykut, 1977; Grenfell, 1979) was used to compute reflection and

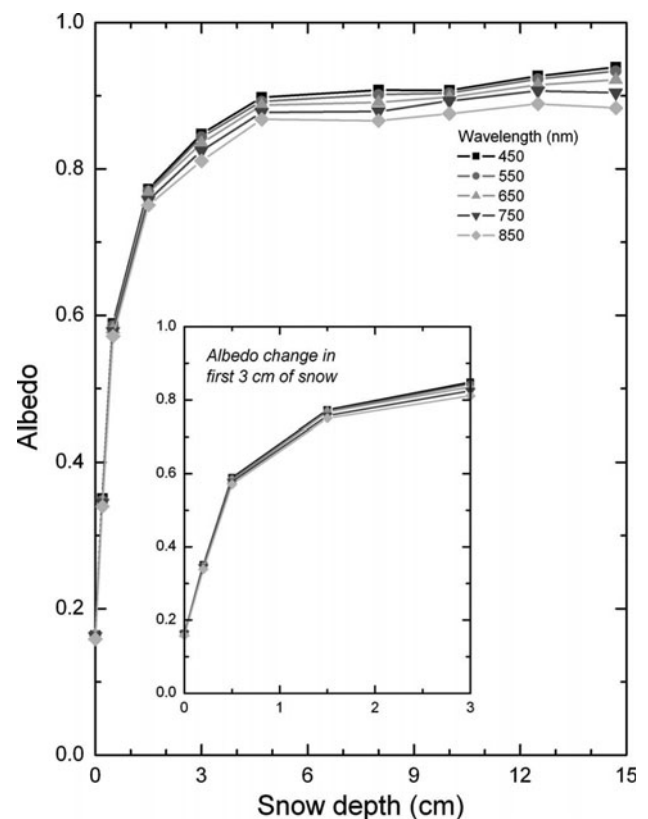


Fig. 3. The increase of spectral albedo as a function of snow depth during the snowfall shown in Figure 2.

extinction coefficients from observed albedos and transmittances. The spectral dependence was also evident in the two-stream extinction coefficients (Fig. 4c), where values ranged from a minimum of 0.05 cm^{-1} at 470 nm to 0.35 cm^{-1} at 875 nm. According to Warren and others (2006), the minimum at 470 nm denotes the presence of impurities. The reflection coefficient was 1.44 cm^{-1} . These extinction coefficients have a spectral shape similar to those reported by Grenfell and Maykut (1977) for Arctic snow, but are approximately one-third the magnitude. The Grenfell and Maykut (1977) values were also computed using the Dunkle and Bevens formulation. This difference is due, in part, to the smaller density (120 kg m^{-3}) of the Hanover snow compared to the Arctic (400 kg m^{-3}) snow.

Transmittance profiles

On a few occasions, when the snow was dry and loosely aggregated, it was possible to remove snow from the platform, layer by layer, using a 3 m long aluminum beam. The beam could be adjusted to different heights, allowing different amounts of snow to be removed while maintaining a level surface. Spectral incident, reflected and transmitted irradiances were measured after the removal of each layer, generating profiles of transmittance as a function of snow depth. Figure 5 shows results at selected wavelengths for one such set of measurements. The snowpack in this case was homogeneous, consisting of a mix of about 25% needles, 1–1.25 mm long, and 75% rounded grains, 0.5–1 mm in diameter, with an average density of 150 kg m^{-3} . The sky was completely overcast and the solar disk was not visible. Transmittance as a function of snow depth is plotted on a semi-log scale in Figure 5a. For all snow thicknesses, the

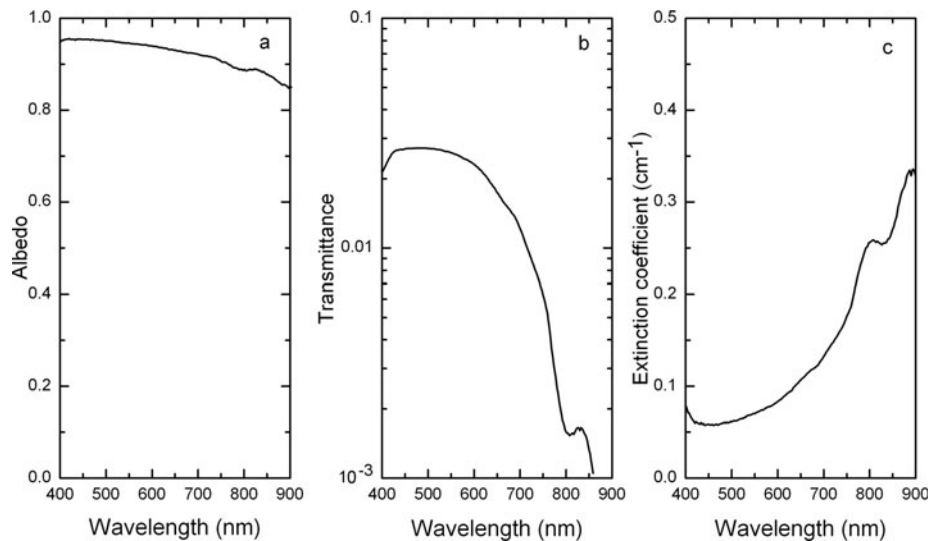


Fig. 4. Spectral (a) albedo, (b) transmittance and (c) extinction coefficient for a 19 cm deep snowpack.

transmittance was greatest at 500 nm. Transmittance decreased with increasing snow depth and at a faster rate for wavelengths beyond 500 nm.

The slope of the curves is the irradiance extinction coefficient, κ in Equation (6). Slopes, and therefore extinction coefficients, were computed for two regions of Figure 5a: snow depths from 2 to 4 cm and from 7 to 12 cm. Extinction coefficients computed for the 2–4 cm snow depth range (Fig. 5b) were larger at all wavelengths than the 7–12 cm values, even though the snowpack appeared to be uniform in its physical properties. This was because the 2–4 cm snow cover was optically thin and was in the non-asymptotic regime, where irradiance losses are greater (Warren, 1982).

Impact of new snow

Even a thin layer of new snow can change the albedo and transmittance of an existing snow cover. Figure 6 explores the case of a 14 cm thick, month-old snowpack composed mainly of rounded grains 0.5–1.0 mm in diameter, with an average density of 200 kg m^{-3} . The top 2 cm of this snowpack was a crust of frozen aggregated sleet with individual

rounded grains that were 1–3 cm in diameter. A brief snowfall deposited a 1.5 cm thick layer of new, fluffy, dendritic snow on top. The new snow had little effect on visible albedos, but did enhance albedos in the near-infrared (Fig. 6a) by as much as 0.06. The 10% increase in total snow depth caused by the new snow resulted in roughly a 20% decrease in transmittance (Fig. 6b). There was a corresponding increase in the overall extinction coefficient for the snowpack with the new snow present (Fig. 6c), and the reflection coefficient increased, from 0.60 to 0.65 cm^{-1} , with the addition of the new snow.

Impact of snowmelt

It is well established that melting causes a reduction in snow albedo (Grenfell and Maykut, 1977; Warren, 1982). The impact of melting on snow albedo, transmittance and extinction coefficient was investigated by observing a snow layer before and after melt. On 12 January 1996 the platform was covered by 14.5 cm of dry snow. The snow cover consisted of two layers. The top 5 cm was ice columns a few millimeters long, with a density of 113 kg m^{-3} . The bottom

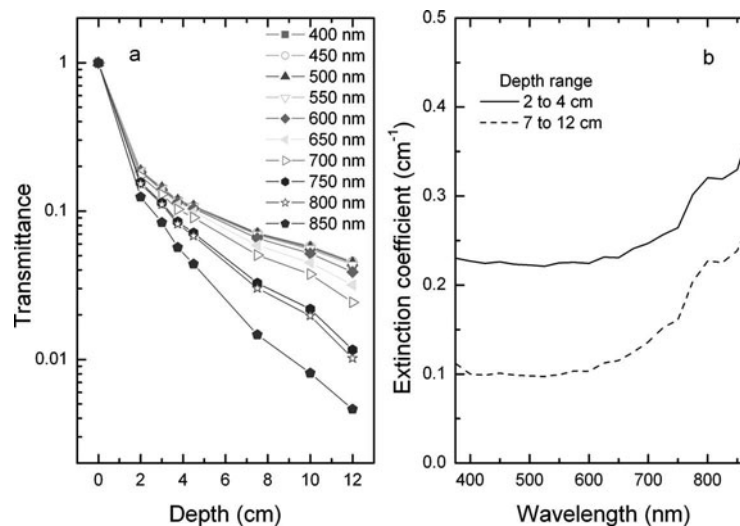


Fig. 5. (a) Profiles of downwelling irradiance as a function of snow depth. (b) Spectral extinction coefficients determined from the slope of the curves in (a).

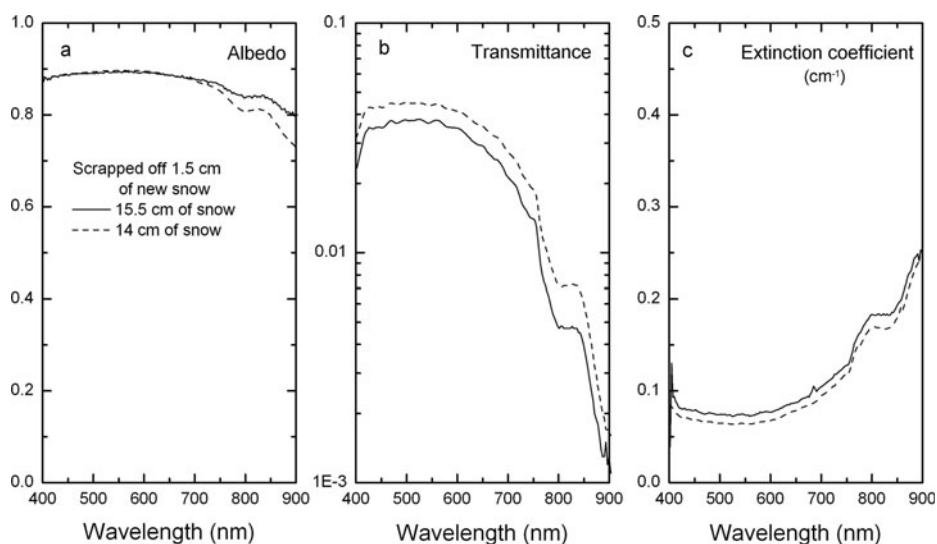


Fig. 6. Impact of a thin layer of new snow on spectral (a) albedo, (b) transmittance and (c) extinction coefficient.

layer was 1–3 mm diameter rounded grains with a density of 159 kg m^{-3} . A few days later, temperatures climbed above freezing and it rained. In response to the rain and above-freezing air temperatures, the snowpack had thinned to 11 cm by 18 January and consisted of rounded grains 0.5–1 mm in diameter saturated in water. The density was 439 kg m^{-3} near the surface, 300 kg m^{-3} in the middle and 337 kg m^{-3} in the bottom layer of the snow.

Because of the water in the 18 January snow cover, many of the ice/air interfaces were changed to ice/water interfaces. The index of refraction contrast at an ice/water interface is much less than at an ice/air interface, reducing scattering. This is evident in the spectral albedos plotted in Figure 7a. Across the spectrum, the albedo of the wet snow was 0.1–0.2 less than that of the dry snow. The reflection coefficient prior to melt was 1.06 cm^{-1} . Because of the reduced scattering in the wet melting snow, the reflection coefficient decreased to 0.84 cm^{-1} on 18 January. Transmittance decreased at all wavelengths, even though the snowpack thinned from 14.5 to 11 cm and the albedo was less. This was a direct result of increased absorption in the snow due

to the large increase in the density. Although the snowpack thinned from 14.5 to 11 cm, the total mass of ice and water (average density multiplied by snow depth) doubled. Extinction coefficients at visible wavelengths were more than a factor of two larger for the wet, denser snow than for the dry snow. There was also a spectral shift to 590 nm in the minimum extinction coefficient for the wet snow, suggesting the presence of contaminants in the snow.

Spectral extinction coefficients

Over the course of the experiment, extinction coefficients were determined for many different snow covers. Figure 8 summarizes results from 20 cases divided into three categories: new snow, older snow and wet melting snow. New snow was less than 1 day old, older snow was more than 1 day old and wet snow was isothermal at the melting point with liquid water present. These plots illustrate both the mean values and the observed variability of extinction coefficients for these categories. New snow and older snow extinction coefficients had the same spectral shape, with new snow values being slightly larger. As new fluffy snow

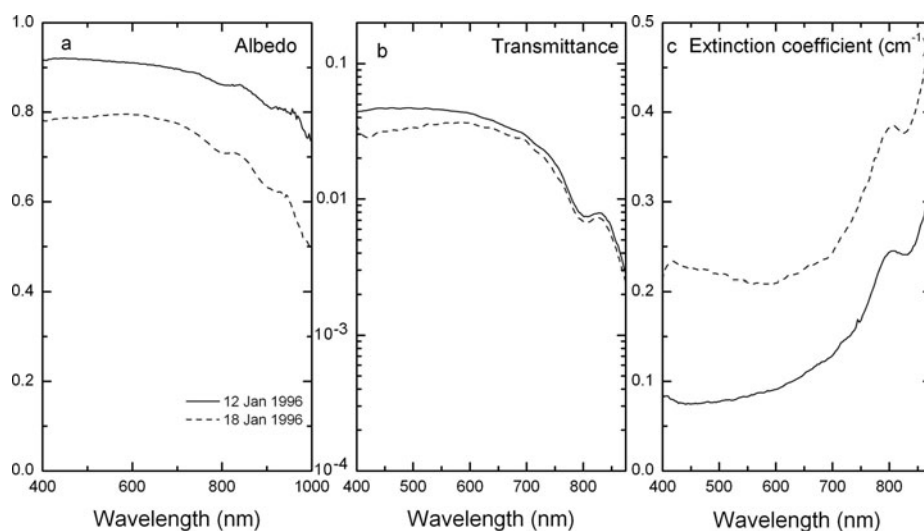


Fig. 7. Impact of snowmelt on spectral (a) albedo, (b) transmittance and (c) extinction coefficient.

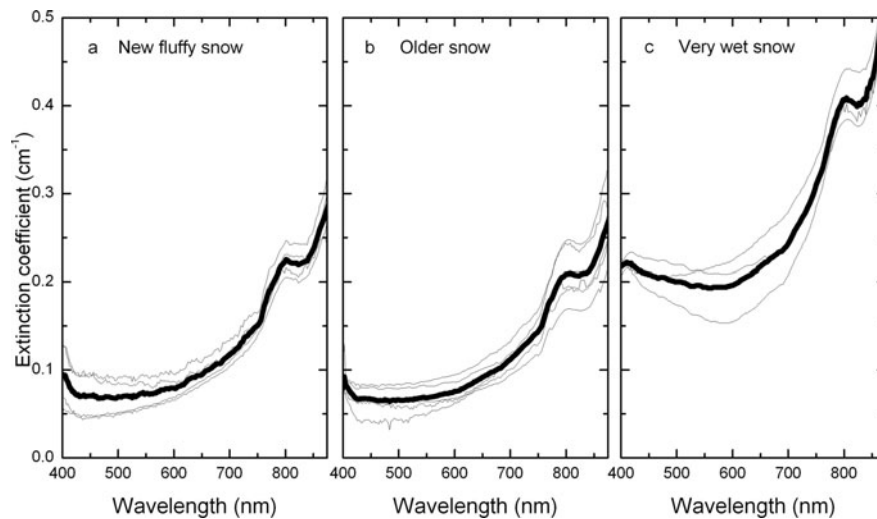


Fig. 8. Range of spectral extinction coefficients for (a) new snow, (b) older snow and (c) melting snow. The heavy line shows the mean extinction coefficient.

metamorphosed into old snow, there was a slight decrease in the extinction coefficient. Wet snow, with the largest densities, had the largest extinction coefficients: more than a factor of two greater than those of new or old snow. For the new and older snow cases, the smallest spectral extinction coefficients and greatest transmittances were typically 450–550 nm. For very wet snow, the minimum extinction coefficient was shifted to 590 nm, implying the presence of particulates and vegetative detritus. For a particular snow type, the relative variability was greatest at shorter wavelengths, where absorption was smaller and the impact of scattering greater. The variation was typically about $\pm 0.04 \text{ cm}^{-1}$ around the mean.

Density

Earlier work (Warren and Wiscombe, 1980; Warren, 1982) established a clear relationship between snow grain size and optical properties. Less clear is the relationship between density and optical properties. Some previous observations have hinted at such a connection, but the density may have been merely a proxy for a different physical property, such as grain size. Bohren and Beshta (1979) examined compacted and uncompacted snow and found no relationship between albedo and density. This relationship is explored in Figure 9, which shows scattergrams of snow density vs extinction coefficients at 450 and 750 nm. Also plotted is snow density

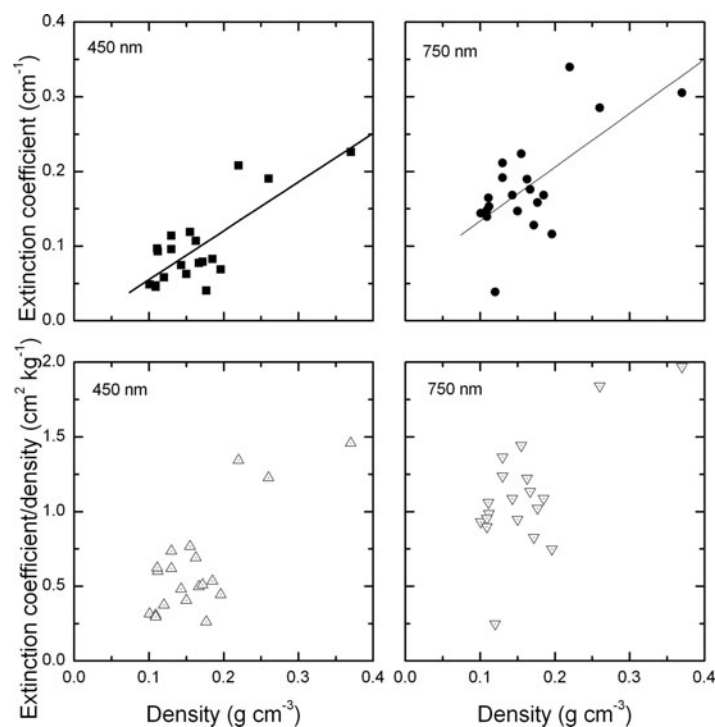


Fig. 9. Top: scattergrams of extinction coefficient vs density at 450 and 750 nm. Bottom: scattergrams of extinction coefficient normalized by density vs density at 450 and 750 nm.

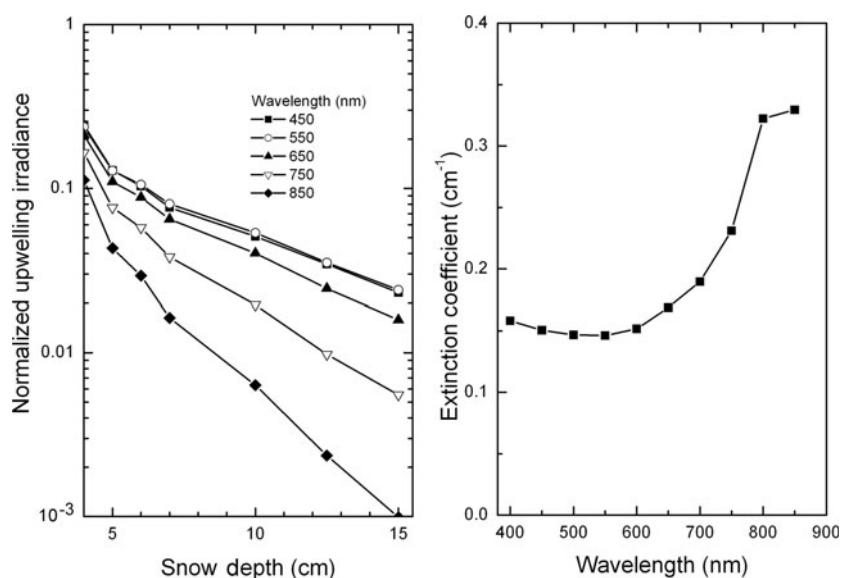


Fig. 10. Profiles of upwelling irradiance measured in a 25 cm deep snowpack.

vs the extinction coefficient divided by density. These plots remove the impact of the additional mass. There is a weak trend towards increasing extinction coefficient with density driven by a few high-density points. There is considerable scatter, particularly for densities of 100–200 kg m⁻³, where most of the data lie and extinction coefficients varied by a factor of 3. The plots where extinction coefficient is divided by density show no relationship. This indicates the presence of other factors, such as grain size, that contribute significantly to extinction.

DISCUSSION

The snow-platform experiments provided a means of investigating the reflection and transmission of light by relatively thin, undisturbed, temperate snowpacks. Snow albedos increased rapidly and asymptotically as the snow depth increased. Visible albedos reached 0.9 for a snow depth of only 5 cm. Transmitted light levels were small, even for thin snow covers. A 10 cm thick snow layer typically reduced visible transmittance to <5% and near-infrared transmittance to <1%. Extinction coefficients at visible wavelengths ranged from 0.05 to 0.3 cm⁻¹ and reflection coefficients varied from 0.60 to 1.44 cm⁻¹. The largest extinction coefficients were for melting snow that was saturated with water. The presence of water in the snowpack reduced the albedo and increased absorbed light.

For all of its strengths, the observational method used in this study is inherently limited, since it is fixed in space and must wait for snowfall. This makes it difficult to survey a wide variety of snow types or to examine the spatial variability of snow optical properties. To address these concerns, an apparatus was developed to allow optical measurements of a snowpack with minimal disturbance. A dual-detector fiber-optic-based spectroradiometer was used (Analytical Spectral Devices Ice-1). One detector is used to monitor the incident irradiance. The second fiber-optic probe, with cosine collector, is mounted on a rod and lowered looking downward into a 5 cm diameter hole in the snow. Measurements are made at selected depths, giving profiles of upwelling transmittance. By changing the

foreoptics it is also possible to measure other parameters, such as downwelling irradiance, spherical irradiance and radiance. A suite of measurements takes only a few minutes and the system is portable, facilitating surveys of transmittance. The in-snow sensor is small (2 cm in diameter), reducing its impact on the radiation field. Two-dimensional Monte Carlo models are available to examine in detail, and adjust for the impact of the small hole and sensor on the radiation field in the snow (Light and others, 2003).

This system was field-tested on a 25 cm deep snowpack in Hanover, NH. The snowpack was dry and had densities of 130 kg m⁻³ in the top half and 290 kg m⁻³ in the bottom half. Profiles of upwelling irradiance are plotted in Figure 10, along with exponential extinction coefficients. The extinction coefficients range from 0.14 to 0.33 cm⁻¹, with a minimum between 500 and 550 nm.

In the future a profiling system could be used to expand investigations of light transmission in and under a snow cover. This system will facilitate the study of a wide range of snow types and conditions. It will also permit detailed measurements in the non-asymptotic regime of the top few centimeters of the snowpack. Additional modeling could be done with irradiance profile data and with results such as the spectral albedos and transmittances reported here, for example, further exploring scattering coefficients and phase functions for snow. These inherent optical properties could then be related to snow physical properties such as density, grain size and crystal type.

ACKNOWLEDGEMENTS

This work has been funded by the Department of the Army basic research program. Thanks to J. Govoni, B. Elder, L. Perovich and C. Perovich for their assistance in making the observations.

REFERENCES

- Askebjerg, P. and 35 others. 1997. Optical properties of deep ice at the South Pole: absorption. *Appl. Opt.*, **36**(18), 4168–4180.
- Barry, R.G. 1996. The parameterization of surface albedo for sea ice and its snow cover. *Progr. Phys. Geogr.*, **20**(1), 63–79.

- Beaglehole, D., B. Ramanathan and J. Rumberg. 1998. The UV to IR transmittance of Antarctic snow. *J. Geophys. Res.*, **103**(D8), 8849–8858.
- Bohren, C.F. and B.R. Barkstrom. 1974. Theory of the optical properties of snow. *J. Geophys. Res.*, **79**(30), 4527–4535.
- Bohren, C.F. and R.L. Beschta. 1979. Snowpack albedo and snow density. *Cold Reg. Sci. Technol.*, **1**(1), 47–50.
- Brandt, R.E. and S.G. Warren. 1993. Solar-heating rates and temperature profiles in Antarctic snow and ice. *J. Glaciol.*, **39**(131), 99–110.
- Chandrasekhar, S.C. 1960. *Radiative transfer*. New York, Dover.
- Dunkle, R.V. and J.T. Bevans. 1956. An approximate analysis of the solar reflectance and transmittance of a snow cover. *J. Meteorol.*, **13**(2), 212–216.
- Gerland, S. and 6 others. 1999. Physical and optical properties of snow covering Arctic tundra on Svalbard. *Hydrol. Process.*, **13**(14), 2331–2343.
- Gerland, S., G.E. Liston, J.G. Winther, J.B. Örbæk and B.V. Ivanov. 2000. Attenuation of solar radiation in Arctic snow: field observations and modelling. *Ann. Glaciol.*, **31**, 364–368.
- Giddings, J.C. and E. LaChapelle. 1961. Diffusion theory applied to radiant energy distribution and albedo of snow. *J. Geophys. Res.*, **66**(1), 181–189.
- Grenfell, T.C. 1979. The effects of ice thickness on the exchange of solar radiation over the polar oceans. *J. Glaciol.*, **22**(87), 305–320.
- Grenfell, T.C. 1991. A radiative transfer model for sea ice with vertical structure variations. *J. Geophys. Res.*, **96**(C9), 16,991–17,001.
- Grenfell, T.C. and G.A. Maykut. 1977. The optical properties of ice and snow in the Arctic Basin. *J. Glaciol.*, **18**(80), 445–463.
- Grenfell, T.C. and D.K. Perovich. 1981. Radiation absorption coefficients of polycrystalline ice from 400–1400 nm. *J. Geophys. Res.*, **86**(C8), 7447–7450.
- Grenfell, T.C. and D.K. Perovich. 1984. Spectral albedos of sea ice and incident solar irradiance in the southern Beaufort Sea. *J. Geophys. Res.*, **89**(C3), 3573–3580.
- Grenfell, T.C., D.K. Perovich and J.A. Ogren. 1981. Spectral albedos of an alpine snowpack. *Cold Reg. Sci. Technol.*, **4**(2), 121–127.
- Grenfell, T.C., S.G. Warren and P.C. Mullen. 1994. Reflection of solar radiation by the Antarctic snow surface at ultraviolet, visible, and near-infrared wavelengths. *J. Geophys. Res.*, **99**(D9), 18,669–18,684.
- Grenfell, T.C., B. Light and M. Sturm. 2002. Spatial distribution and radiative effects of soot in the snow and sea ice during the SHEBA experiment. *J. Geophys. Res.*, **107**(C10), 8032. (10.1029/2000JC000414.)
- Grenfell, T.C., S.P. Neshyba and S.G. Warren. 2005. Representation of a nonspherical ice particle by a collection of independent spheres for scattering and absorption of radiation: 3. Hollow columns and plates. *J. Geophys. Res.*, **110**(D17), D17203. (10.1029/2005JD005811.)
- Hamre, B., J.-G. Winther, S. Gerland, J.J. Stamnes and K. Stamnes. 2004. Modeled and measured optical transmittance of snow-covered first-year sea ice in Kongsfjorden, Svalbard. *J. Geophys. Res.*, **109**(C10), C10006. (10.1029/2003JC001926.)
- Jin, Z. and J.J. Simpson. 2001. Anisotropic reflectance of snow observed from space over the Arctic and its effect on solar energy balance. *Remote Sens. Environ.*, **75**(1), 63–75.
- Kokhanovsky, A.A. and E.P. Zege. 2004. Scattering optics of snow. *Appl. Opt.*, **43**(7), 1589–1602.
- Kou, L.H., D. Labrie and P. Chylek. 1993. Refractive indices of water and ice in the 0.65 to 2.5 μm spectral range. *Appl. Opt.*, **32**(19), 3531–3540.
- Light, B. 2000. Structural–optical relationships in first-year sea ice. (PhD thesis, University of Washington.)
- Light, B., G.A. Maykut and T.C. Grenfell. 2003. A two-dimensional Monte Carlo model of radiative transfer in sea ice. *J. Geophys. Res.*, **108**(C7), 3219. (10.1029/2002JC001513.)
- McKenzie, R.L., K.J. Paulin and S. Madronich. 1998. Effects of snow cover on UV irradiance and surface albedo: a case study. *J. Geophys. Res.*, **102**(D22), 28,785–28,792.
- Mishchenko, M.I., J.M. Dlugach, E.G. Yanovitskij and N.T. Zakharova. 1999. Bidirectional reflectance of flat, optically thick particulate layers: an efficient radiative transfer solution and applications to snow and soil surfaces. *J. Quant. Spectrosc. Radiat. Transfer*, **63**(2–6), 409–432.
- Nolin, A.W. and J. Stroeve. 1997. The changing albedo of the Greenland ice sheet: implications for climate modeling. *Ann. Glaciol.*, **25**, 51–57.
- Nolin, A.W., K. Steffen and J. Dozier. 1994. Measurement and modeling of the bidirectional reflectance of snow. In Stein, T.I., ed. *Proceedings of International Geoscience and Remote Sensing Symposium (IGARSS 1994), August 8–12, 1994*. Piscataway, NJ, Institute of Electrical and Electronics Engineers, 1919–1921.
- Painter, T.H. and J. Dozier. 2004. Measurements of the hemispherical-directional reflectance of snow at fine spectral and angular resolution. *J. Geophys. Res.*, **109**(D18), D18115. (10.1029/2003JD004458.)
- Perovich, D.K. 1990. Theoretical aspects of light reflection and transmission by spatially complex and temporally varying sea ice covers. *J. Geophys. Res.*, **95**(C6), 9557–9567.
- Perovich, D.K. and T.C. Grenfell. 1982. A theoretical model of radiative transfer in young sea ice. *J. Glaciol.*, **28**(99), 341–356.
- Smith, R.C. and 12 others. 1992. Ozone depletion: ultraviolet radiation and phytoplankton biology in Antarctic waters. *Science*, **255**(5047), 952–959.
- Stamnes, K., S.C. Tsay, W. Wiscombe and K. Jayaweera. 1988. Numerically stable algorithm for discrete-ordinate-method radiative transfer in multiple scattering and emitting layered media. *Appl. Opt.*, **27**(12), 2502–2509.
- Stroeve, J.C. and A.W. Nolin. 2002. New methods to infer snow albedo from the MISR instrument with applications to the Greenland ice sheet. *IEEE Trans. Geosci. Remote Sens.*, **40**(7), 1616–1625.
- Thomas, W.H. and B. Duval. 1995. Snow algae: snow albedo changes, algal–bacterial interrelationships, and ultraviolet radiation effects. *Arct. Antarct. Alp. Res.*, **27**(4), 389–399.
- Van de Hulst, H.C. 1981. *Light scattering by small particles*. New York, Dover.
- Warren, S.G. 1982. Optical properties of snow. *Rev. Geophys. Space Phys.*, **20**(1), 67–89.
- Warren, S.G. 1984. Optical constants of ice from the ultraviolet to the microwave. *Appl. Opt.*, **23**(8), 1206–1225.
- Warren, S.G. and W.J. Wiscombe. 1980. A model for the spectral albedo of snow. II. Snow containing atmospheric aerosols. *J. Atmos. Sci.*, **37**(12), 2734–2745.
- Warren, S.G., R.E. Brandt and P. O’Rawe Hinton. 1998. Effect of surface roughness on bidirectional reflectance of Antarctic snow. *J. Geophys. Res.*, **103**(E11), 25,789–25,805.
- Warren, S.G., R.E. Brandt and T.C. Grenfell. 2006. Visible and near-ultraviolet absorption spectrum of ice from transmission of solar radiation into snow. *Appl. Opt.*, **45**(21), 5320–5334.
- Wiscombe, W.J. and S.G. Warren. 1980. A model for the spectral albedo of snow. I. Pure snow. *J. Atmos. Sci.*, **37**(12), 2712–2733.
- Wolff, E.W., J.S. Hall, R. Mulvaney, E.C. Pasteur, D. Wagenbach and M. Legrand. 2002. Modelling photochemical NO_x production and nitrate loss in the upper snowpack of Antarctica. *Geophys. Res. Lett.*, **29**(20), 1944. (10.1029/2002GL015823.)